Molecular Therapy
Nucleic Acids
Original Article

Characterization of Long Noncoding RNA and mRNA Profiles in Sepsis-Induced Myocardial Depression

Tie-Ning Zhang,[1] Julie E. Goodwin,[2,3] Bing Liu,[2,3] Da Li,[4] Ri Wen,[1] Ni Yang,[1] Jing Xia,[1] Han Zhou,[2,3] Tao Zhang,[1] Wen-Liang Song,[1] and Chun-Feng Liu[1]

[1]Department of Pediatrics, PICU, Shengjing Hospital of China Medical University, Shenyang, Liaoning Province, 110004, China; [2]Department of Pediatrics, Yale University School of Medicine, New Haven, CT, USA; [3]Department of Vascular Biology and Therapeutics Program, Yale University School of Medicine, New Haven, CT, USA; [4]Department of Obstetrics and Gynecology, Shengjing Hospital of China Medical University, Shenyang, China

Septic shock with heart dysfunction is very common in intensive care units. However, whether long noncoding RNA (lncRNA) and mRNA profiles differ between patients with and without myocardial depression is unknown. We generated rat models of hypodynamic septic shock induced by lipopolysaccharide. A total of 12 rat models was constructed and heart tissue from each was collected. Whole genomic RNA sequencing was performed on left ventricular tissue; 6,508 novel lncRNAs and 432 annotated lncRNAs were identified in heart samples, and 74 lncRNAs were expressed differently in the sepsis and control groups. Gene ontology term enrichment indicated apoptosis and its related pathways showed obvious enrichment, which suggested cell apoptosis could play a critical role in the process of myocardial depression. Furthermore, we focused on one lncRNA from the Pvt1 gene. By silencing this lncRNA, we demonstrated knockdown of Pvt1 expression could induce cell apoptosis in lipopolysaccharide-induced heart cells, through increasing the expression of c-Myc, Bid, Bax, and caspase-3 and decreasing the expression of Myd88 and Bcl-2, thereby proving its functional role in myocardial depression. These results demonstrate that lncRNAs both participate in and mediate the pathological process of myocardial depression. Our study improves the understanding of the basic molecular mechanisms underlying myocardial depression.

INTRODUCTION

Sepsis is a syndrome of physiological, pathological, and biochemical abnormalities caused by the altered systemic host response to infection.[1,2] Septic shock is a subset of sepsis, in which underlying circulatory and cellular abnormalities are profound enough to greatly increase mortality.[1] Notably, the myocardial dysfunction during sepsis is usually called sepsis-induced myocardial depression or sepsis-induced heart dysfunction,[3] characterized by impaired myocardial contractility and reduced ejection fraction.[3,4] This phenomenon can lead to higher mortality, especially in pediatric septic shock patients.[5] However, the underlying molecular mechanism of sepsis-induced myocardial depression remains unclear.

Recent studies indicate that microRNAs (miRNAs) are involved in the process of sepsis-induced myocardial depression.[6] Long noncoding RNAs (lncRNAs) are a type of noncoding RNA with a length exceeding 200 nt. These lncRNAs contribute to transcriptional and post-transcriptional functions, and they can be broadly classified either as signaling molecules, decoy molecules, guide molecules, or scaffold molecules.[7] Unlike miRNAs, which have been extensively studied, the lncRNAs present in sepsis-induced myocardial depression have never been sequenced. As is well known, next-generation sequencing has become a powerful approach that can reveal different expression profiles underlying phenotypic differences, as well as decipher non-annotated transcriptional activity by identifying various novel transcripts (protein-coding and noncoding) and additional alternative splice variants of known annotated transcripts.[8,9] The limited number of identified lncRNAs in sepsis-induced myocardial depression may impede further study of its complex molecular mechanism.

Therefore, we hypothesized that lncRNAs are involved in the pathological process of sepsis-induced myocardial depression. The present study aimed to describe the features of lncRNAs and mRNAs in sepsis-induced myocardial depression. Furthermore, we focused on one particular lncRNA (transcript ID: ENSRNOT00000092896, gene ID: ENSRNOG00000062170, and gene name: Pvt1) for further research, which was the transcript from the rat Pvt1 gene. Our study provides a useful resource to study the functional roles of lncRNA and link the characteristic lncRNAs and mRNAs to myocardial depression phenotypes.

Received 10 April 2019; accepted 24 July 2019;
https://doi.org/10.1016/j.omtn.2019.07.020.

Correspondence: Chun-Feng Liu, Department of Pediatrics, PICU, Shengjing Hospital of China Medical University, No. 36, SanHao Street, Shenyang, Liaoning 110004, China.
E-mail: zhliu258@hotmail.com

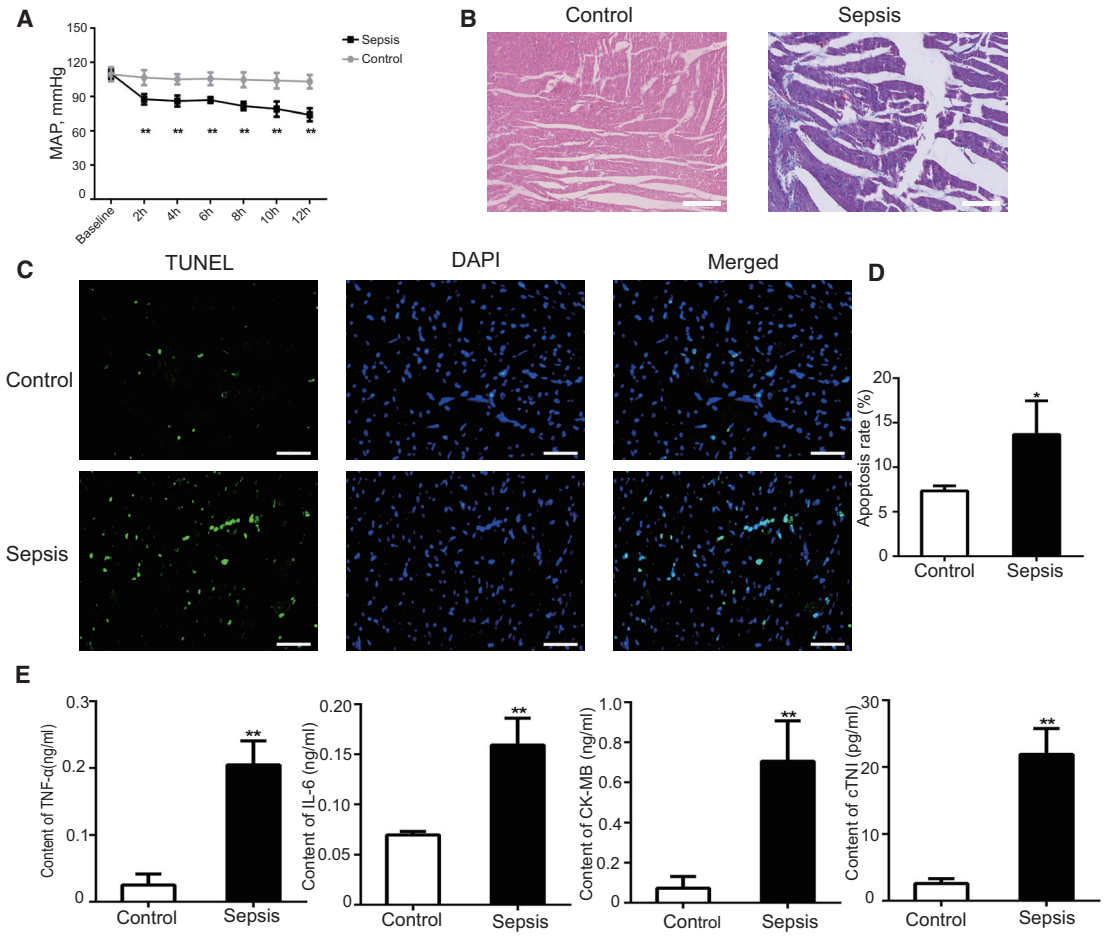

Figure 1. Basic Characteristics of Animal Models between Septic Shock Group and Control Group

(A) *In vivo* mean arterial pressure (MAP) hemodynamic studies. n = 6 in each group. (B) Pathological comparation in heart tissue by H&E staining (10×). (C and D) Apoptosis detection in heart tissue by TUNEL staining (400×). n = 3 in each group. (E) Serum inflammatory biomarker (TNF-α and IL-6) and cardiac enzyme (cTnI and CK-MB) levels were detected by ELISA. n = 6 in each group; *p < 0.05 compared to the control; **p < 0.01 compared to the control.

RESULTS

Model Identification of Myocardial Depression in Rats with Septic Shock

Our previous study showed that there is a positive relationship between mean arterial pressure (MAP) and heart function.[10] Therefore, we measured MAP and found that MAP started to decline approximately 1.5 h after the administration of LPS. Septic shock occurred approximately 2 h after LPS administration, and it lasted for the rest of the observation period (Figure 1A). In the control group, MAP appeared unchanged throughout the entire observation period. Furthermore, H&E staining showed that there was infiltration of inflammatory cells and rupture of myocardial cells in hearts of the septic rats compared to those in the control group (Figure 1B). Terminal deoxynucleotidyl transferase-mediated dUTP nick-end labeling (TUNEL) staining of heart tissue showed a statistically significant increase in apoptosis rates in septic shock animals (Figures 1C and 1D). Finally, we examined serum inflammatory biomarkers (tumor necrosis factor-α [TNF-α] and interleukin-6 [IL-6]) and cardiac enzymes (cardiac troponin I [cTnI] and creatine kinase MB form [CK-MB]) (Figure 1E), and we found that all of these were significantly elevated in the septic animals.

RNA Sequencing Identified the Features of lncRNA and mRNA in Myocardial Depression of Septic Shock

We analyzed RNA sequencing (RNA-seq) data from 12 rat heart samples, in which 82,000,000–115,000,000 raw data and 79,000,000–110,000,000 clean data were obtained (Table 1). The classification of mapped reads in each heart tissue is shown in Figure S1. After comparing the SNP, insertion or deletion (indel), and alternative splicing (AS) events in the sepsis and control groups, we found that the SNP and indel counts in sepsis were less than those in the control group, although there were no obvious differences in AS events (Figure S2).

Table 1. The Detailed Information of RNA Sequencing

Sample	Raw Reads	Clean Reads	Clean Bases (G)	Error Rate (%)	Q20 (%)	Q30 (%)	Total Mapped (%)
Control 1	104,887,116	101,842,730	15.28	0.01	98.09	95.02	96.42
Control 2	110,482,096	107,303,972	16.10	0.01	98.17	95.17	96.62
Control 3	109,101,010	105,976,634	15.90	0.01	98.20	95.27	96.41
Control 4	114,063,808	110,459,742	16.57	0.01	98.30	95.49	96.55
Control 5	104,412,260	101,257,002	15.19	0.01	98.11	95.06	96.22
Control 6	102,114,088	99,322,108	14.90	0.01	98.17	95.20	96.43
Sepsis 1	85,541,078	82,755,500	12.41	0.02	97.22	92.88	95.85
Sepsis 2	83,814,640	80,941,514	12.14	0.02	96.87	92.16	95.48
Sepsis 3	92,375,116	90,576,722	13.59	0.01	97.21	93.01	95.09
Sepsis 4	82,418,946	79,773,136	11.97	0.02	97.13	92.70	95.91
Sepsis 5	101,060,828	98,158,896	14.72	0.01	98.08	94.99	96.43
Sepsis 6	115,144,142	110,000,016	16.50	0.02	97.22	92.90	95.68

To minimize the false-positive rate in identifying lncRNAs from 287,301 assembled transcripts, we developed a filtering flowchart to discard transcripts without all characteristics of lncRNA (Figure 2A). By this method, we identified 6,508 novel lncRNAs from an intersection of the analysis results of CPC, CNCI, and PFAM (Figures 2B and 2C), which included 4,642 lncRNAs (71.3%), 979 antisense lncRNAs (15.0%), and 887 intronic lncRNAs (13.6%) (Figure 2D). We compared the number of overlapping lncRNAs in the sepsis and control groups, which suggested that the lncRNAs that appeared in the sepsis group also appeared in the control group (Figure 2E). There were 23,010 mRNAs included in our study, and we compared the number of overlapping mRNAs in the sepsis and control groups (Figure 2F). In addition, our study found that annotated and novel lncRNAs had a smaller size, fewer exons, and fewer open reading frames than mRNAs (Figures 2G–2I). However, there was no significant difference in transcript levels in heart tissue from the sepsis and control groups (Figures 2J–2L).

Differential Expression and Cluster Analysis of lncRNAs and mRNAs

To check if lncRNAs were involved in the pathological process of sepsis-induced myocardial depression, the expression patterns of lncRNAs and mRNAs were analyzed. We analyzed differential expression (DE) lncRNAs and mRNAs using significance analysis following the criterion $q < 0.05$. As a result, there were 74 DE lncRNAs (33 upregulated and 41 downregulated) and 4,011 DE mRNAs (1,918 upregulated and 2,093 downregulated) (Figures 3A and 3B). The expression pattern of DE lncRNAs and mRNAs is shown using a cluster heatmap (Figures 3C and 3D).

In addition, among all DE lncRNAs, there were 35 annotated lncRNAs and 39 novel lncRNAs, and their relative levels of expression are shown in Figures 3E and 3F. There was one novel downregulation lncRNA (LNC_006245) that was not detected in the sepsis group. The detailed information of the top 10 upregulated and 10 downregulated lncRNAs is summarized in Table S1, and the top 20 upregulated and 20 downregulated mRNAs are summarized in Table S2. The relative expression levels of several prominent DE mRNAs are shown in Figure 3G. These results reflect distinct lncRNA and mRNA expression profiles between sepsis-induced myocardial depression and the control group, implying different underlying pathophysiology in sepsis-induced heart dysfunction.

Systematic Functional Analysis of Differentially Expressed lncRNAs and mRNAs

To elucidate the possible functional significance of observed changes in lncRNA and mRNA levels between sepsis-induced myocardial depression and the control group, we performed a Gene Ontology (GO) term enrichment analysis. There were 20,121 background genes in total. We summarized the significantly enriched GO terms of lncRNAs (Figures 4A–4C) and mRNAs (Figures 4D–4F) regarding biological process, cellular component, and molecular function, respectively. Notably, the number of enriched genes at the lncRNA level was much less than that at the mRNA level regarding biological process. Interestingly, the differentially expressed lncRNAs and mRNAs were similar and significantly associated with regulation and metabolic processes in biological process term enrichment (Figures 4A and 4D). Importantly, the GO term RNA metabolic process was a significant enrichment on both the lncRNA and mRNA levels, which indicates that noncoding RNAs and mRNAs could make sense in the pathological process of sepsis. It is noteworthy that cell apoptosis and cell death were enriched in both lncRNAs and mRNAs, suggesting that cell apoptosis and cell death might play a critical role in sepsis-induced myocardial depression.

In addition, the enrichment of cellular components and molecular function also showed a similar pattern. For example, molecular-bounded organelle, intracellular part, and nucleus were all obviously enriched on the lncRNA and mRNA levels (Figures 4B and 4E). For molecular function enrichment, terms regarding binding such as

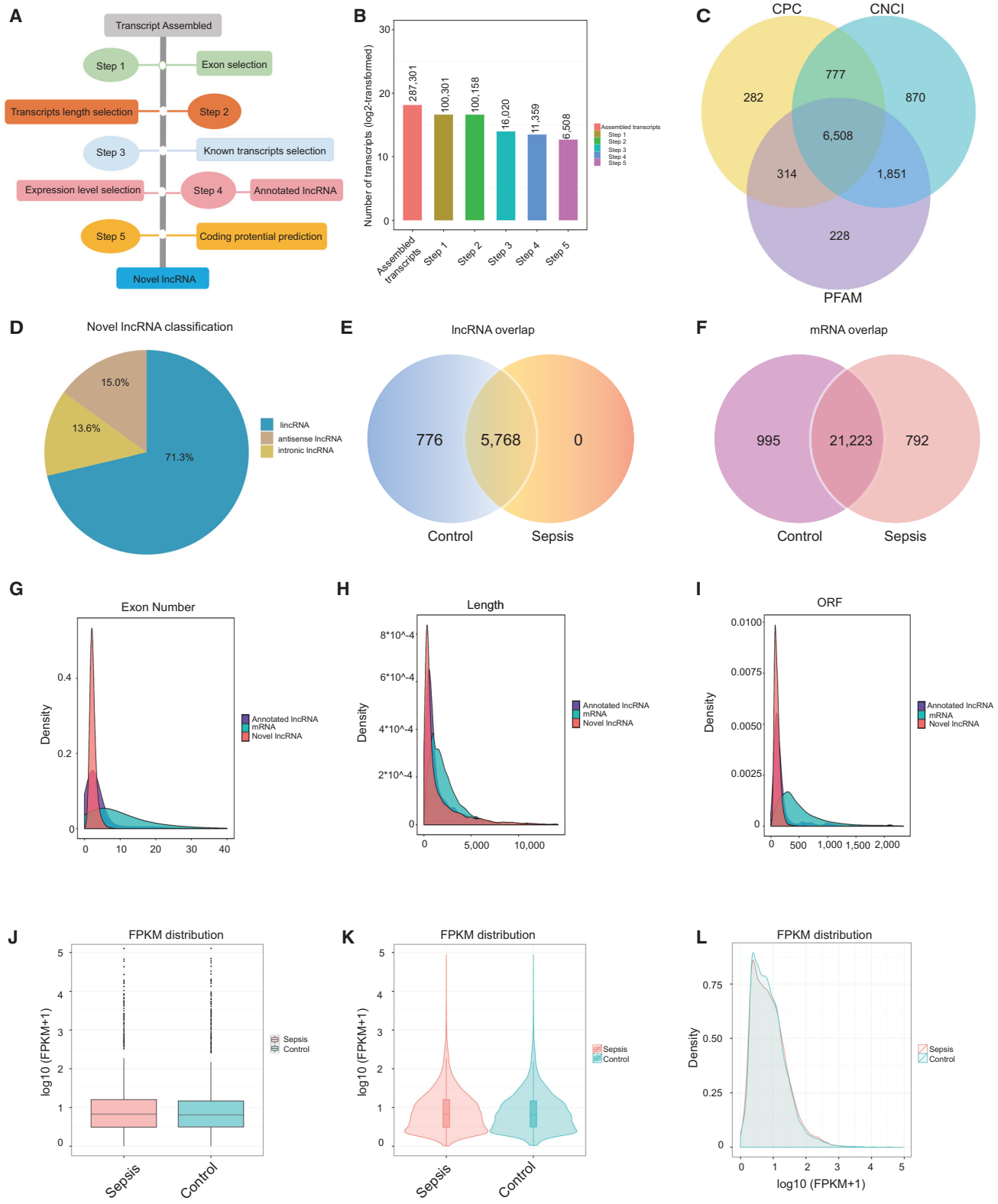

(legend on next page)

protein binding and enzyme binding were enriched, which suggested that complex pathological processes are involved in sepsis-induced myocardial depression.

To determine if there were some specific pathways changed in sepsis, we performed the Kyoto Encyclopedia of Genes and Genomes (KEGG) enrichment analysis in lncRNA target genes and mRNAs. Interestingly, the apoptosis pathway was also enriched in both lncRNAs and mRNAs, which is consistent with the GO term enrichment results (Figures 4G and 4H). Therefore, we performed further chromosomal localization, and we analyzed the interactions and co-expression of genes in apoptosis-related pathways, at the lncRNA, lncRNA-mRNA, and mRNA levels, respectively (Figures 4I–4K). The TNF-signaling pathway,[11,12] nuclear factor κB (NF-κB)-signaling pathway,[13,14] and Jak-Stat pathway[15,16] were enriched, which previous studies have implicated in sepsis-induced myocardial depression; our KEGG enrichment analysis also suggested their significance.

Validation of DE lncRNAs by qPCR

According to the KEGG pathway enrichment analysis and previous sepsis studies, we concluded that the following pathways might be relevant in sepsis-induced myocardial depression: TNF-signaling pathway,[11,12] NF-κB-signaling pathway,[13,14] Jak-Stat pathway,[15,16] and apoptosis pathway.[17,18] To validate the reliability of the sequencing results and to provide the basis for further study, five annotated (ENSRNOT00000000787, ENSRNOT00000092896, ENSRNOT00000086178, ENSRNOT00000091713, and ENSRNOT 00000076955) and four novel (LNC_001626, LNC_004326, LNC_004590, and LNC_004777) DE lncRNAs were chosen to analyze by qPCR, which included at least one target gene that appeared in the aforementioned four common pathways (Figure 5).

To detect widespread DE lncRNAs in sepsis-induced myocardial depression, we expanded the sample numbers (n = 15 in each group) for validation using our previous heart tissue samples. All lncRNAs selected for validation were statistically significant and consistent with the results obtained from next-generation sequencing, which indicated the high quality and validity of RNA-seq.

The Role of lncRNA rPvt1 in Sepsis-Induced Myocardial Depression

By considering GO terms, KEGG pathway enrichment, and our findings using the septic shock model, we found that apoptosis could be a critical factor in myocardial depression. The *Pvt1* gene and its related lncRNAs have been reported in research in humans, which suggested that this gene was related to cell apoptosis.[19,20] We focused on an lncRNA from *Pvt1*, which was named lncRNA rPvt1 for further study. Surprisingly, the fold changes from qPCR and RNA-seq were almost the same and showed significant upregulation in the sepsis group. In addition, we realized that its target genes included several classical apoptosis-related genes, such as *Myc*, *p53*, *Bid*, and *Myd88* (Figure S3), which is highly suggestive of a potential role in the apoptosis process.

We first located its expression area by RNA fluorescence *in situ* hybridization (FISH) in the H9c2 cell line after LPS administration, and we noticed that lncRNA rPvt1 could express in both the nucleus and cytoplasm (Figure 6A). In addition, we performed northern blot to evaluate its total sequence length, and we found that the expression bands were near the second shortest marker (representing the length of 1,821 bp) (Figure 6B). To validate the sequence accuracy and acquire its total length, we conducted rapid amplification of cDNA ends (RACE) clone experiments twice: the first time RACE clone was used to test the known sequence and acquire the 3′ end and 5′ end sequence, and the second RACE test aimed to demonstrate the acquired total sequence and show congruence. Similar to the results of the northern blot, we acquired an unknown 91-bp sequence from the 5′ end RACE and an unknown 325-bp sequence from the 3′ end RACE (Figure 6C).

To elucidate the potential role of lncRNA rPvt1 in apoptosis, we first detected that lncRNA rPvt1 showed upregulation in the LPS-induced H9c2 cell line compared with the control group (Figure 6Di), which was consistent with the result from animal models. We then performed lentivirus transfection to silence this lncRNA, and we observed that its expression level was clearly decreased (Figure 6Dii). Furthermore, we performed the detection of cell apoptosis and cell cycle in four groups, including a control group, LPS-induced group, LPS-induced negative control (NC) group, and LPS-induced knockdown (KD) group. We found that the apoptosis rates increased significantly in the LPS-induced cells compared with the control group after 24 and 48 h. As for the LPS-induced NC and KD groups, the cell apoptosis rate increased in the silencing group compared with the NC group following LPS administration after 24 and 48 h, respectively (Figure 6E).

Regarding cell cycle analyses, we noticed that there was a decreasing trend of S phase cells in the LPS-induced group compared with normal cells, and there was also an obvious decrease of S phase cells in the LPS-induced KD group compared with the NC group after 48 h (Figure 6F). We also performed cell counting kit-8 (CCK-8) to determine both the proliferation ability in the control and LPS

Figure 2. Characterization of lncRNAs and mRNAs in Rat Heart Tissue

(A and B) The five steps of novel lncRNA screening. (C) Coding potential analysis via CPC, PFAM, and CNCI. Those sequences simultaneously shared by the above three tools were selected as candidate lncRNAs. (D) The classification of identified lncRNAs. (E) Venn diagram showing the number of overlapping lncRNAs in sepsis group compared with control group. (F) Venn diagram showing the number of overlapping mRNAs in sepsis group compared with control group. (G–I) Density distribution diagram showing the expression features of exon number (G), length (H), and opening reading frame (ORF) (I) of annotated lncRNAs, novel lncRNAs, and mRNAs in rat heart tissue. (J–L) Boxplot (J), violin plot (K), and density distribution diagram (L) showing the expression features of rat heart tissue from the sepsis group and the control group. FPKM, fragments per kilobase million.

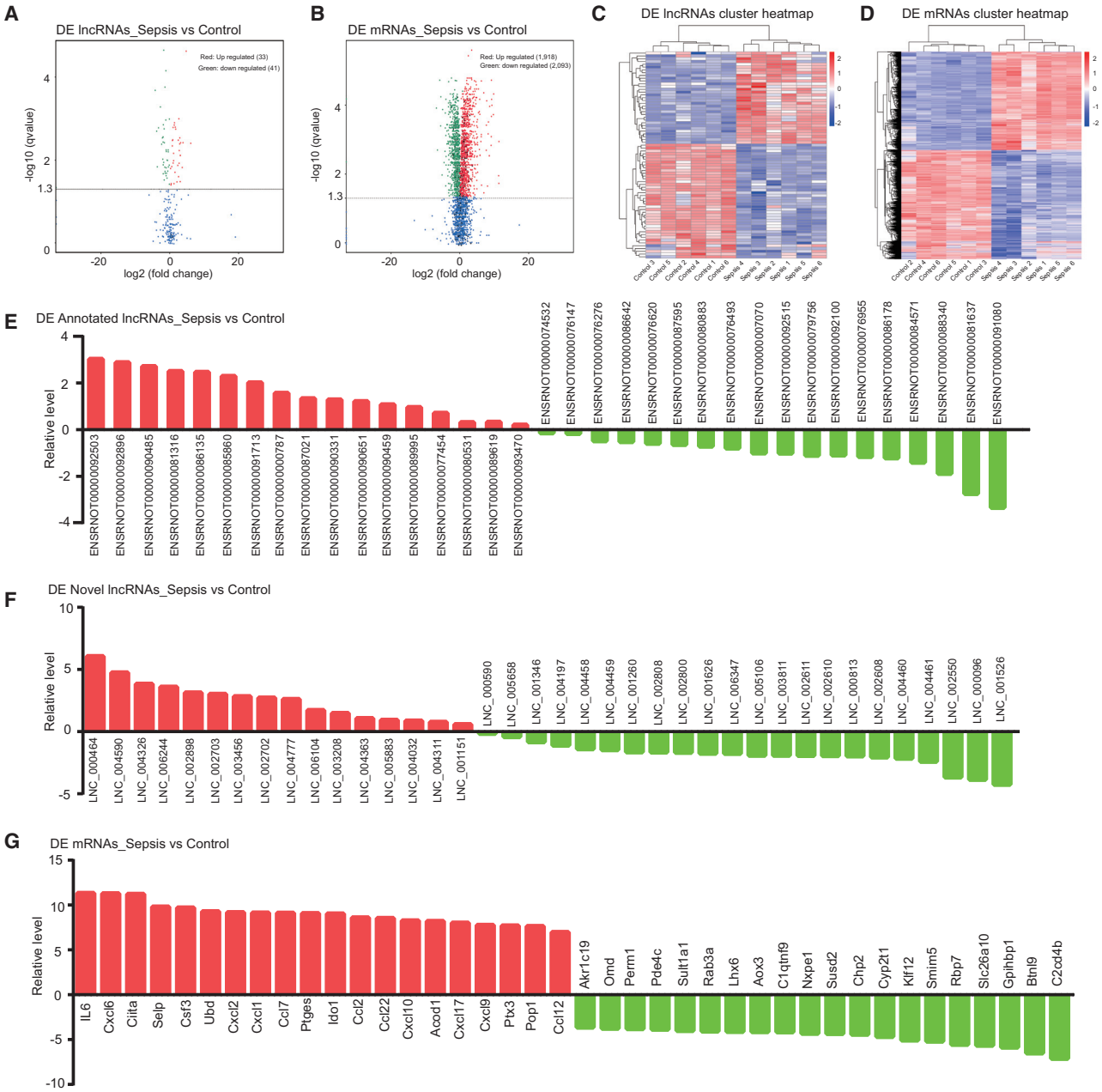

Figure 3. The Expression Profiling Changes of lncRNAs and mRNAs in Rat Heart Tissue

(A and B) Volcano plot indicating up- and downregulated lncRNAs (A) and mRNAs (B) of rat heart tissue in the sepsis group compared with the control group; up- and downregulated genes are colored in red and blue, respectively. (C and D) Heatmap of lncRNAs (C) and mRNAs (D) showing hierarchical clustering of changed lncRNAs and mRNAs of rat heart tissue in the sepsis group compared with the control group; up- and downregulated genes are colored in red and blue, respectively. (E–G) Differences in the expressions of annotated lncRNAs (E), novel lncRNAs (F), and mRNAs (G) in rat heart tissue from the sepsis and normal groups. DE, differential expression.

administration groups and the influence of lncRNA rPvt1 on cell proliferation. This showed that there was a statistically significant difference between the control and LPS administration groups at 24, 36, and 48 h (Figure 6Gi). Additionally, proliferation in the knockout (KO) group was decreased compared with the NC group after LPS administration at both 36 and 48 h (Figure 6Gii). However, the absolute difference of estimated values in these two groups was less than 20%, which suggests that our results provide limited evidence that lncRNA rPvt1 can influence cell proliferation in LPS-induced H9c2 cells.

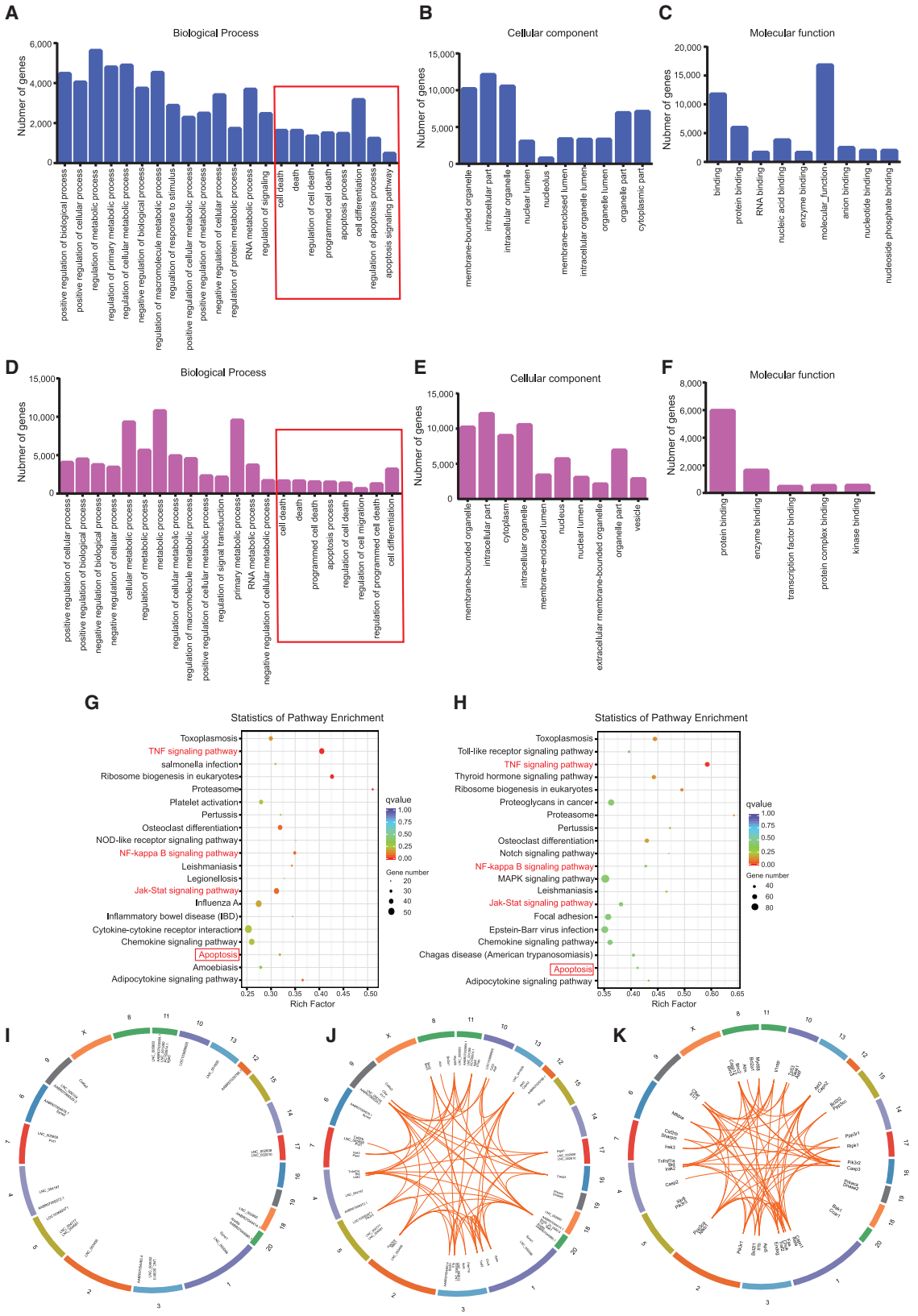

(legend on next page)

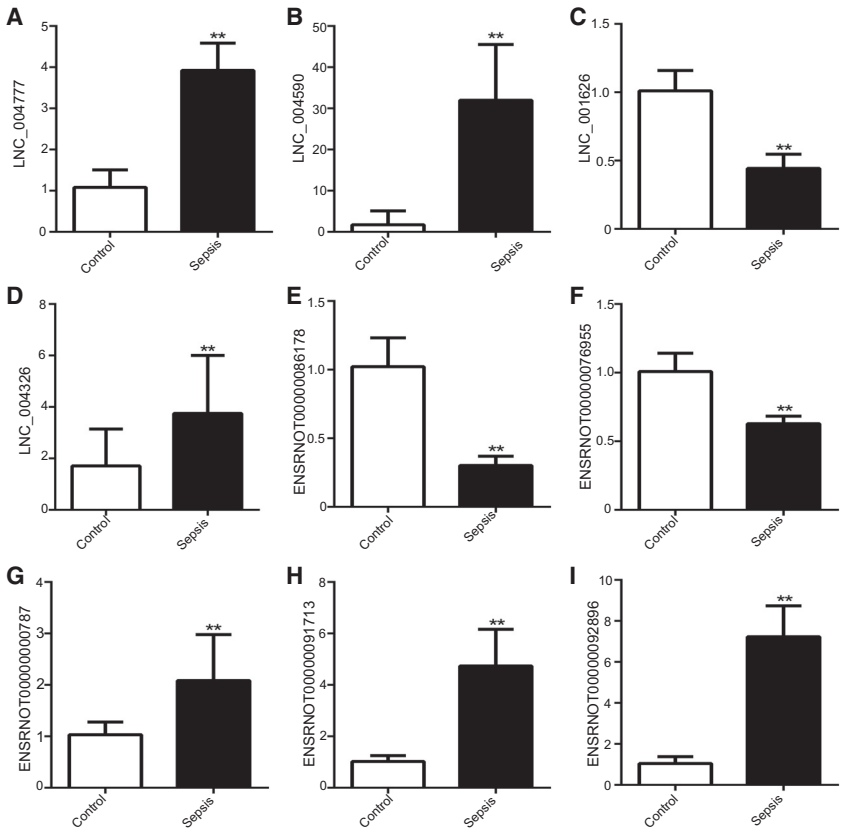

Figure 5. qPCR Validations

(A–I) qPCR validations of nine regulated lncRNAs in rat heart tissue from the sepsis group and the control group. n = 15 in each group; **p < 0.01 compared to the control.

The Potential Mechanism of lncRNA rPvt1 in the Regulation of Cell Apoptosis

We identified that major target genes of lncRNA rPvt1 relating to apoptosis included *Myd88*, *c-Myc*, *Bid*, and *p53*. As such, we investigated the changes in these four proteins and other apoptosis-related proteins, such as Bax, Bcl-2, and caspase-3, in heart tissue from control and sepsis groups, using immunohistochemistry (IHC) and western blot. We found that the protein expressions of Myd88, c-Myc, cleaved-Bid, Bax, and cleaved-caspase-3 significantly increased and the expression of Bcl-2 obviously decreased in the sepsis group compared with the control group. However, there was no difference in the p53 protein between the control and sepsis groups (Figures 7A and 7B). Furthermore, to illustrate which genes were regulated and influenced by lncRNA rPvt1, we performed western blot of these proteins in a control cell line, an LPS-induced cell line, an LPS-induced NC group, and an LPS-induced KD group (Figure 7C). We noticed that the Myd88 and Bcl-2 proteins decreased in the LPS-induced KD group but that the expressions of c-Myc, cleaved-Bid, Bax, and cleaved-caspase-3 increased compared with the LPS-induced NC group.

Additionally, we performed RNA pull-down combined with mass spectrographic analysis to analyze whether the proteins were involved in the regulation process of lncRNA rPvt1 (Figure 7D). We found that the Irak-2 protein, which participates in the IL-1R/Myd88 pathway, could bind directly with lncRNA rPvt1 in the sepsis group, but not in the control group. Furthermore, we proved that the expressions of Irak-2 and IL-1R were different in the control and sepsis groups (Figure 7Ei) and that, after silencing lncRNA rPvt1, the expression of Irak-2 obviously decreased in the LPS-induced KD group compared with the LPS-induced NC group (Figure 7Eii). These results suggest that the IL-1R/Myd88/Irak-2 pathway could be involved in septic myocardial depression and that lncRNA rPvt1 might influence Myd88 through binding with the Irak-2 protein.

DISCUSSION

Sepsis, as a clinical emergency, usually causes multi-organ dysfunction and can lead to high mortality.[21] Despite improvements in intensive care treatments, septic shock, which is a subtype of sepsis with circulatory and cellular and/or metabolic dysfunction, is still associated with a higher risk of mortality. Unlike warm shock with high-cardiac output and low peripheral vascular resistance occurring in adult septic shock, pediatric septic shock often occurs as cold shock and is characterized by low cardiac output and high peripheral vascular resistance. Therefore, it is necessary to understand the mechanisms of myocardial depression and aim to reduce the mortality in clinic. To reflect and simulate the pathological process of pediatric septic shock, which is usually modeled by cecal ligation and puncture,

Figure 4. GO and KEGG Analyses of Differentially Expressed lncRNA Target Genes and mRNAs in Rat Heart Tissue from the Sepsis Group and the Control Group

(A–C) GO categories (biological process, A; cellular components, B; and molecular function, C) of differential lncRNA target genes in rat heart tissue from the sepsis group and the control group. (D–F) GO categories (biological process, D; cellular components, E; and molecular function, F) of differential mRNAs in rat heart tissue from the sepsis group and the control group. (G) KEGG analysis of differential lncRNA target genes in rat heart tissue from the sepsis group and the control group. (H) KEGG analysis of differential mRNAs in rat heart tissue from the sepsis group and the control group. (I–K) RCircos package analysis displaying chromosomal localization and the interactions of the co-expression of genes (STRING) regarding apoptosis-related pathways at the lncRNA level (I), lncRNA-mRNA level (J), and mRNA level (K).

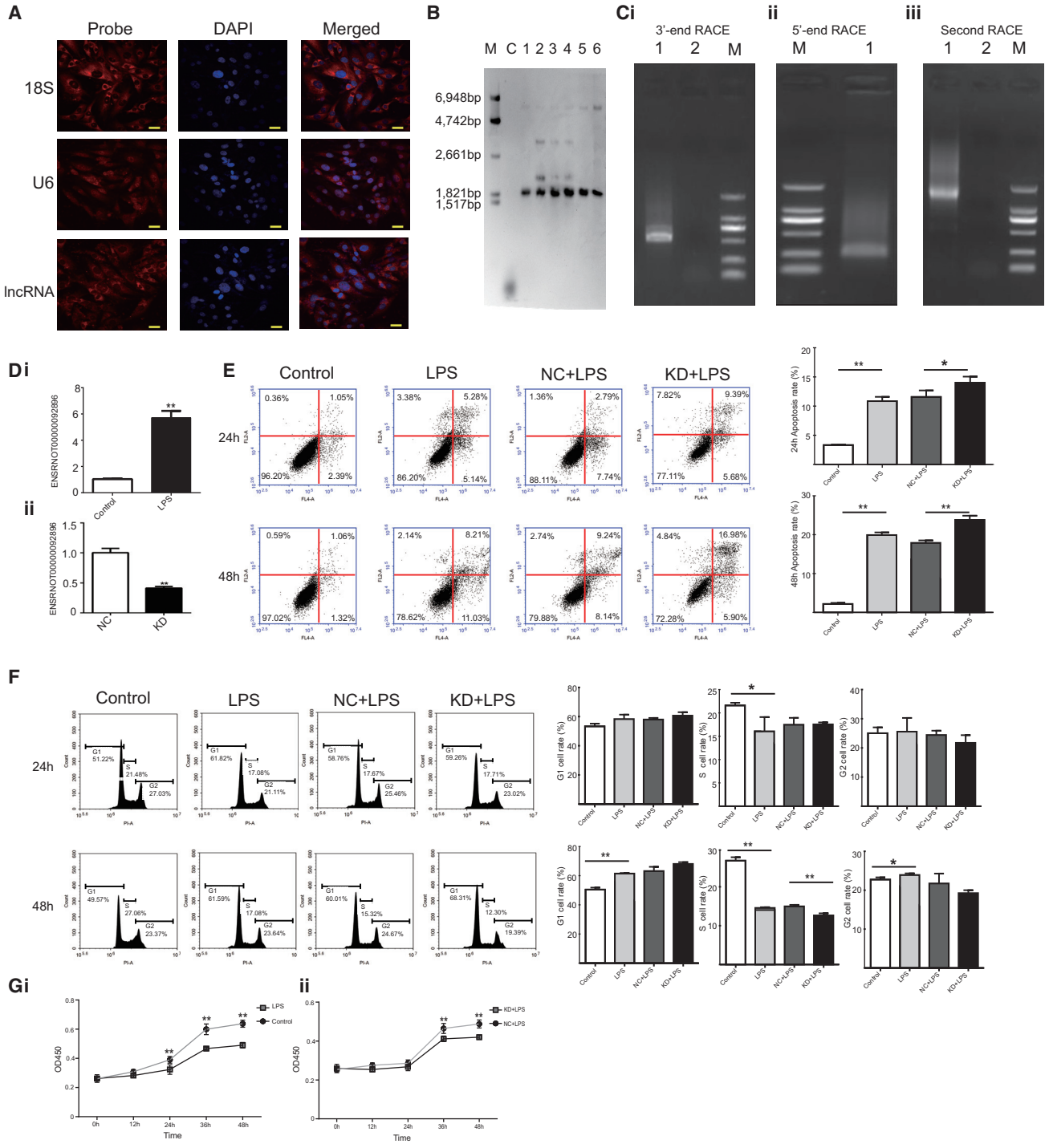

Figure 6. Functional Study of lncRNA rPvt1

(A) Expression location of lncRNA rPvt1 in LPS-induced H9c2 cell lines by fluorescence *in situ* hybridization (FISH) under confocal microscopy (600×). (B) The expression of lncRNA rPvt1 detected by northern blot (M, marker; C, positive control product; bands 1–3, heart tissue from the control group; bands 4–6, heart tissue from the sepsis group). (C) Rapid amplification of cDNA ends (RACE) to acquire the total sequence of lncRNA rPvt1 (i, 3′ end RACE; M, marker; 1, 3′-RACE inner PCR product (+); 2, 3′-RACE inner PCR product (–); ii, 5′ end RACE; M, marker; 1, PCR product; iii, second RACE for validation; M, marker; 1, validation PCR product [+];

(legend continued on next page)

we used a rat model subjected to a high dose of LPS, which showed an obvious and rapid shock and accompanying myocardial dysfunction. Our model is relatively stable and has a high reproducibility rate; therefore, it is suitable for studying the mechanism of septic shock in children.

Recently, with the development of next-generation high-throughput sequencing, multiple lncRNAs have been identified and shown to play important roles in many diseases.[22,23] Compared with microarray, next-generation sequencing has many strengths, including high sensitivity and specificity, and the ability to discover important novel lncRNAs. However, there is no relevant study using whole genomic sequencing that reports and compares changes in lncRNAs and mRNAs in sepsis-induced myocardial depression.

To realize the basic characteristics of lncRNAs and mRNAs and evaluate the potential role of lncRNAs in septic myocardial depression, our study identified entire lncRNAs and mRNAs changing significantly in left ventricular tissues compared with the non-sepsis group. In addition, to improve the reliability and validity of sequencing, we developed six septic shock animals compared with six control animals to find the ubiquitous DE lncRNAs and mRNAs. According to quality control and qPCR validation, our sequencing results had high reliability and quality. Through bioinformatics analysis, we predicted potential functions of lncRNAs and mRNAs by GO term enrichment and KEGG pathway enrichment, and we found important changes that help us to understand the molecular mechanisms of sepsis-induced myocardial depression more clearly. In addition, we focused on one specific lncRNA, lncRNA rPvt1, and we conducted several experiments to thoroughly investigate its characteristics and evaluate its potential role in cell function. Our study indicates that lncRNAs, including lncRNA rPvt1, play important roles in the pathological process of septic myocardial depression and provide a new direction toward understanding this pathological process.

We identified 74 DE lncRNAs between sepsis and control groups; the underlying mechanisms of these lncRNAs are poorly understood. We also performed GO enrichment and found that the terms of biological processes occupied most of the significantly enriched terms. According to our KEGG enrichment results, we found that TNF-signaling pathway, NF-κB-signaling pathway, Jak-Stat pathway, and apoptosis pathway were the common pathways that appeared at both the lncRNA and mRNA levels. Although some published studies[11,14,16,17] stated the potential role of the aforementioned four common pathways in sepsis, the regulatory relationship between lncRNAs and these pathways is still unclear and should be studied in more depth in future basic studies.

Although a recent study conducted by Takasu et al.[24] showed that myocardial tissue from patients with sepsis lacked significant necrosis, apoptosis, or autophagy compared with control donor hearts, we detected a significant difference in both apoptosis rates and the levels of several proteins related to cell apoptosis, including Myd88, c-Myc, Bid, Bax, Bcl-2, and caspase-3, in heart tissue from the septic shock and control groups. These results are also consistent with the results of GO term and KEGG pathway enrichment. To realize the co-expression relationships of genes relating to the apoptosis pathway, we also performed gene analyses of chromosomal localization and regulatory association between lncRNA and mRNA. We detected an obvious rate of apoptosis, which is partly due to the fact that we performed the septic shock model with a large dose of LPS, producing a more serious subtype of sepsis characterized by severe heart dysfunction and damage. In the previous clinical study,[24] the included patients were septic patients rather than those in septic shock, which might explain why they did not develop serious myocardial damage. Another potential explanation is that we used a pediatric septic shock model, which has a different pathological process compared to adult sepsis. The low cardiac output in pediatric sepsis may reflect a severely impaired heart function, whereas there is usually normal or high cardiac output in adult sepsis. Therefore, apoptosis could be an important mechanism of heart dysfunction in pediatric septic shock.

We also focused on one particular lncRNA and estimated its role in a septic model in cell culture. From previous studies, we knew that the lncRNA from human *Pvt1* could regulate the apoptosis process. For example, a study conducted by He et al.[20] showed that silencing lncRNA Pvt1 could increase cell apoptosis in nasopharyngeal carcinomas, and other studies support this notion in different malignancies.[19,25] Although the sequence of lncRNA rPvt1 is different from that lncRNA from the human Pvt1 gene, we speculated that our lncRNA could influence and regulate cellular function in heart tissue through bioinformatics analysis. Therefore, to evaluate the potential role of lncRNA rPvt1 in sepsis, we created a lentiviral vector and silenced lncRNA, after which we observed that knockdown of *Pvt1* expression could induce cell apoptosis in the LPS-induced heart cell line. This result suggests that *Pvt1* could play a role in sepsis-induced myocardial depression.

Compared with the control group, lncRNA rPvt1 in the sepsis group had a tendency toward high expression levels, and therefore this lncRNA could have a protective effect in sepsis. Furthermore, we evaluated the influence of lncRNA rPvt1 on its potential target genes, and we found that lncRNA rPvt1 could regulate the expression of several genes, including Myd88, c-Myc, and Bid, and then further influence the expression of genes related to cell apoptosis, such as Bax, Bcl-2, and caspase-3. Notably, in cancer-related research, several studies[26,27] had reported that Pvt1 controls levels of Myc through regulation of

2, validation PCR product [−]). (D) Expression level of lncRNA rPvt1 in control and LPS-induced H9c2 cell line (i); detection of knock down rate by qPCR after lentiviral transfection for silencing lncRNA rPvt1 (ii). (E) Apoptosis detection in H9c2 cell line by flow cytometry. (F) Cell cycle detection in H9c2 cell line by flow cytometry. (G) Proliferation detection in control and LPS-induced cell lines (i), LPS-induced NC cell line, and LPS-induced KD cell line (ii) by CCK-8. NC, negative control group; KD, lncRNA rPvt1 knockdown group; *$p < 0.05$ compared to the control; **$p < 0.01$ compared to the control.

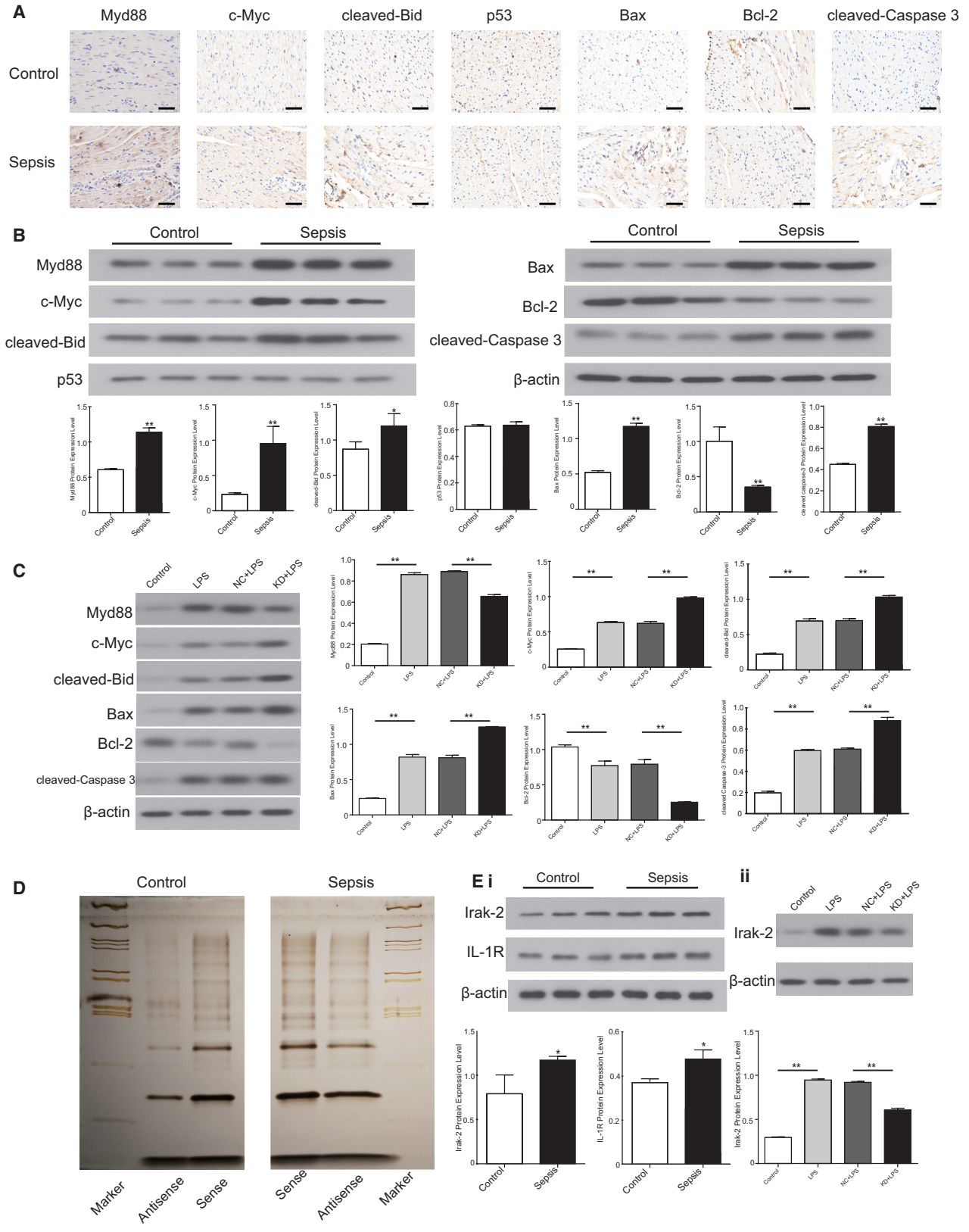

(legend on next page)

the protein's stability. However, there was no prior study focusing on the role of lncRNA rPvt1 in heart tissue in sepsis. In our study, we found that silencing lncRNA rPvt1 could increase both the protein level of c-Myc and the expressions of Bax and caspase-3, therefore increasing cell apoptosis in rat heart tissue.

Our results also showed that the expression of Myd88 decreased in the LPS-induced KD group compared with the LPS-induced NC group. After performing RNA pull-down, we hypothesized that this process might be mediated by Irak-2, which could bind with lncRNA rPvt1 directly, and that the IL-1R/Myd88/Irak-2 pathway might be involved in this process. Although silencing lncRNA rPvt1 could inhibit the expression of Myd88 and Irak-2, which would decrease the inflammatory response to a certain extent, in fact we found that silencing lncRNA rPvt1 led to an increase in cell apoptosis. This effect may be explained by a greater relative increase in other apoptosis-related proteins, such as Bax and Bid, and a decrease in the anti-apoptotic protein Bcl-2. However, the mechanism by which lncRNA rPvt1 influences c-Myc and regulates the expressions of Bax, Bid, and caspase-3 still requires further research to fully understand.

Our study is an investigation into the role of lncRNAs in the pathological process of myocardial depression in models of septic shock. By applying whole genomic next-generation sequencing, we compared the DE lncRNAs and mRNAs between sepsis and control groups. These abundant data prompted the proposal that lncRNAs may interact and regulate their related protein-gene expression and, thus, play a key role in the pathogenesis of sepsis-induced myocardial depression. Additionally, we investigated lncRNA rPvt1 and detected its role in the myocardial cell model of sepsis. lncRNAs may provide new insights into the pathophysiology of sepsis-induced myocardial depression, as well as the potential for development of lncRNA mediators in the future.

MATERIALS AND METHODS

Animal Model of Septic Shock

The study was approved by the Ethics Committee of Shengjing Hospital of China Medical University (2019PS073K). All experiments conformed to all relevant regulatory standards. The adolescent rat model of septic shock was generated by intraperitoneal injection of LPS, as in our previous description.[10] Briefly, male pathogen-free Wistar rats from Changsheng Bio (Benxi, China) weighing from 170 to 190 g were anesthetized by 20% urethane (1 g/kg i.p.). We cannulated the left femoral artery to continue monitoring the MAP of the models (Biopac MP150 Biopac Systems, Goleta, CA, USA). After the MAP was stable, we challenged the rat with *Escherichia coli* 055:B5 (L-2880, Sigma-Aldrich, St. Louis, MO, USA; 20 mg/kg, 10 mg LPS dissolved in 1 mL 0.9% saline), and septic shock was established when the MAP decreased to 25%–30% of the baseline value. For the control group, 0.9% saline (2 mL/kg) was injected into the peritoneal cavity of rats. The left ventricle of the heart was excised after 12-h LPS or saline administration and immediately snap frozen in liquid nitrogen and stored at −80°C for further experiments. In addition, we collected blood from the abdominal aorta at 12 h after LPS or saline administration, which was centrifuged (3,000 rpm, 10 min) after being maintained at room temperature for 15 min. The blood supernatant was collected and stored at −80°C for ELISA.

H&E Staining, TUNEL Assay for Apoptosis, and ELISA Determination of Rat Serum

The heart samples were fixed in 10% formaldehyde for 48 h. The specimens were subjected to dehydration and permeabilization and then embedded in paraffin. The paraffin tissues were sliced into serial sections (0.4 μm) and stained with H&E. Pathological changes were observed under a microscope.

We used the TUNEL technique to detect apoptosis of heart tissues. A TUNEL apoptosis assay kit was purchased from WanleiBio (Shenyang, China), and we performed the assay in accordance with the manufacturer's instructions.

We detected TNF-α, IL-6, CK-MB, and cTnI in blood serum according to the instructions of the ELISA kit (CusaBio, Wuhan, China). The concentration of each sample was calculated according to the optical density value and the standard curve.

RNA-Seq and Bioinformatics Analyses

Sequencing data were deposited with the NCBI (Sequence Read Archive [SRA]: PRJNA527717). The procedures regarding sequencing, data processing, and further bioinformatics analyses can be found in detail in the Supplemental Materials and Methods. Total RNAs from rats subjected to septic shock (n = 6) and controls (n = 6) were isolated and quality controlled. The preparation of whole-transcriptome libraries and next-generation sequencing were conducted by Novogene Bioinformatics Technology (Beijing, China). RNA-seq was performed on an Illumina Hiseq 4000 platform, and 150-bp-paired single-end reads were generated according to Illumina's protocol. All the downstream bioinformatics analyses were based on the clean data with high quality.

Validation of Gene Expression in RNA-Seq by qPCR Analysis

Total RNA was isolated from heart tissue or cultured cells, according to the manufacturer's instructions supplied with the TRIzol Reagent

Figure 7. Mechanism Study of lncRNA rPvt1

(A) Immunohistochemical staining of Myd88, c-Myc, cleaved-Bid, p53, Bax, Bcl-2, and cleaved-caspase-3 in rat heart tissue from the control and sepsis groups (400×). n = 3 in each group. (B) Western blot analysis of Myd88, c-Myc, cleaved-Bid, p53, Bax, Bcl-2, and cleaved-caspase-3 in rat heart tissue from control and sepsis rat models. n = 3 in each group. (C) Western blot analysis of Myd88, c-Myc, cleaved-Bid, Bax, Bcl-2, and cleaved-caspase-3 in the normal H9c2 cell line, LPS-induced cell line, LPS-induced NC cell line, and LPS-induced KD cell line. n = 3 in each group. (D) Silver staining of rat heart tissue during RNA pull-down in control and sepsis groups. n = 1 in each group. (E) Western blot analysis of Irak-2 and IL-1R in rat heart tissue (i) and H9c2 cell line (ii). n = 3 in each group; *$p < 0.05$ compared to the control; **$p < 0.01$ compared to the control.

(Invitrogen, Life Technologies, Carlsbad, CA, USA), and then reverse transcribed with a Thermo First Synthesis Kit. Primers of lncRNAs were designed and synthesized by GenechemBio (Shanghai, China). The specific quantitative primers for nine lncRNAs are listed in Table S1. Each targeted cDNA was amplified using SYBR Green via the StepOnePLUS Real-Time PCR system (Applied Biosystems, Waltham, MA, USA). In addition, the primers of the GAPDH gene were designed as an endogenous control.

RACE Clone of lncRNA rPvt1

The PCR and RACE primers were designed and synthesized by Takara Bio (Dalian, China). Total isolated RNA was converted into cDNA using PrimeScript 1st Strand cDNA Synthesis Kit (Takara, 6110A, Japan) with oligo dT primer. All kits used in this section were provided with SMARTer RACE 5′/3′ Kit component (Takara, 634858, Japan). We strictly conducted the 3′-RACE and 5′-RACE PCR reactions that generated the 3′ and 5′ cDNA fragments according to the manufacturer's instructions. Then, purified PCR products were cloned into the pUC-19 vector and sequenced by Takara Bio (Dalian, China).

Northern Blot Analysis

The heart tissues from the septic shock and control groups were used for RNA isolation and detection, run on a 1% agarose gel, and transferred to positively charged nylon membranes. The membranes were subjected to hybridization with 10.0 mL DIG Easy Hyb-labeled probes overnight at 50°C. Then, the band lncRNA rPvt1 was detected with X-ray film in a dark room. The probe sequences for lncRNA rPvt1 gene were 5′-AGATGTTACAAGTGGCCTAATG-3′ (forward) and 5′-AGAGGTCTATCCTTGCTCTTTA-3′ (300 bp) (reverse), which were designed and synthesized by Sangon Bio (Shanghai, China).

Cell Culture and Treatment Protocol

The rat cardiomyoblast H9c2 cell line, obtained from the Shanghai Institute of Biochemistry and Cell Biology (Shanghai, China), was cultured at 37°C under 5% CO_2 in DMEM containing 10% fetal bovine serum with 100 U/mL penicillin and 100 μg/mL streptomycin. Cells were passaged regularly and subcultured to 80% confluence prior to experimental procedures. For a septic cell model,[10] we treated the cell line with LPS (10 μg/mL) for 12, 24, 36, and 48 h.

FISH of lncRNA rPvt1

RNA FISH was performed using a Fluorescent *in situ* Hybridization kit from RiboBio (Guangzhou, China), in accordance with the manufacturer's instructions. We used U6 and 18 s as our endogenous controls, which were obtained from RiboBio. The stained samples were imaged under confocal microscopy.

Lentiviral Silencing of lncRNA rPvt1

The development of a lentiviral vector system to knock down lncRNA rPvt1 expression was designed to express small interfering RNA (siRNA) sequences for targeting Pvt1. A lentiviral vector that carried a nontargeting sequence was used as the NC of siPVT1. To track targeted cells, we designed a co-expressed GFP marker. The sequence of the lncRNA rPvt1 targeting siRNA was as follows: 5′-CCTATGAGGTGATGATAAA-3′. The H9c2 cell line was seeded into 6-well plates for 24 h and subsequently transfected with lentivirus in both the KO and NC groups. The transfected cells were grown at 37°C with 5% CO_2 for 96 h and then used for further experiments.

Measurement of Cell Apoptosis and Cell Cycle

The H9c2 cells were divided into four groups: normal cells, LPS-induced H9c2 cells, and LPS-induced H9c2 cells in the KO and NC groups. All cells were trypsinized and subsequently harvested and incubated using an Annexin V-APC apoptosis detection kit (eBioscience, Waltham, MA, USA) after regular centrifugation and washing. Cellular apoptosis was evaluated via flow cytometry (Phoenix Flow Systems, San Diego, CA, USA) within 5 min and analyzed using a flow cytometer (Coulter EPICS XL-MCL FACScan, BD Biosciences, Franklin Lakes, NJ, USA). The data were analyzed using the guava InCyte Software to determine the cell apoptosis rates.

As for the measurement of cell cycle, cells were stained with a fluorescent dye (propidium iodide) that directly binds to the DNA in the nucleus. After ethanol fixation and centrifugation, cells were then resuspended and 100 μL RNase A (Sigma, St. Louis, MO, USA) was added into each sample. After 30-min incubation at 37°C, 500 μL propidium iodide was added to each tube for at least 30 min to provide the nuclear signal for fluorescence-activated cell sorting (flow cytometry). Finally, cell cycle was evaluated with a flow cytometer.

Cell Proliferation Assay

The cells transfected with siRNA were seeded into 96-well plates (2,000 cells per well), incubated for 24 h, and then treated with LPS. According to the manufacturer's instructions, a CCK-8 (Sigma-Aldrich, St. Louis, MO, USA) was used to determine cell proliferation after LPS stimulation. The absorbance of each well was monitored using a spectrophotometer at a wavelength of 450 nm.

Immunohistochemical Staining

Immunohistochemical staining for Myd88, c-Myc, cleaved-Bid, p53, Bax, Bcl-2, and cleaved-caspase-3 was conducted on the left ventricular tissue from control and sepsis group. The myocardial tissue was deparaffinized and rehydrated in a graded series of alcohol solutions. Sections were treated with 3% H_2O_2 for 30 min to block endogenous peroxidase activity and then with 1% BSA in PBS for 30 min. Slides were incubated overnight at 4°C with primary antibody (Myd88, c-Myc, p53, Bax, and Bcl-2; 1:200; Abcam, Cambridge, MA, USA; cleaved Bid and cleaved-caspase-3; 1:200; WanleiBio, Shenyang, Liaoning Province, China). The secondary antibody with horseradish peroxidase was used for incubation for 1 h. Images were viewed by a bright-field microscope (Nikon).

Western Blot Analysis

The rat heart tissue and cultured H9c2 cell line were homogenized in RIPA buffer. Proteins from the homogenate (20 μg/well) were

separated on a one-dimensional 4%–10% SDS polyacrylamide gel and transferred to a polyvinylidene membrane (Bio-Rad, Hercules, CA, USA) with a semidry electrotransfer apparatus for 1.5 h at 300 mA. The expression levels of Myd88, c-Myc, cleaved-Bid, p53, Bax, Bcl-2, cleaved-caspase-3, Irak-2, and IL-1R were determined (Myd88, c-Myc, p53, Bax, Bcl-2, and IL-1R; 1:1,000; Abcam, Cambridge, MA, USA; Irak-2; 1:1,000; Cell Signaling Technology, Danvers, MA, USA; cleaved Bid and cleaved-caspase-3; 1:500; WanleiBio, Shenyang, Liaoning Province, China). The immunoblots were visualized by enhanced chemiluminescence (ECL detection kit from GE Healthcare, Chicago, IL, USA).

RNA Pull-down Assay

Briefly, biotin-labeled lncRNA rPvt1 and its antisense RNAs from heart tissue in control and sepsis groups were transcribed *in vitro* with the Biotin RNA labeling mix and T7 RNA polymerase, then treated with RNase-free DNase I. All the pull-down experiment was used and followed the protocol from Magnetic RNA-protein Pull-Down Kit (Thermo Fisher, Waltham, MA, USA). Then, the proteins were measured using mass spectrographic analysis.

Statistical Analysis

All experiments were performed at least three times. Data of a normal distribution were presented as the mean ± SEM. The Student's t test for unpaired data was used to compare between the two groups. Two-way ANOVA of repeated measures was used to analyze the data of MAP changes with LPS administration. The statistical analysis was done using SPSS 23.0 software (IBM, Armonk, NY, USA). $p < 0.05$ was considered statistically significant.

SUPPLEMENTAL INFORMATION

Supplemental Information can be found online at https://doi.org/10.1016/j.omtn.2019.07.020.

AUTHOR CONTRIBUTIONS

T.-N.Z. and C.-F.L. conceived and designed the study. T.-N.Z performed most assays. T.-N.Z. and R.W. performed animal models and heart tissue collection. T.-N.Z., T.Z., and W.-L.S. performed qPCR and western blot. T.-N.Z., J.E.G., B.L., D.L., N.Y., J.X., H.Z., and C.-F.L performed RNA-seq data analysis and interpretation. T.-N.Z., J.E.G., B.L., D.L., and C.-F.L. wrote the manuscript. All the authors read and approved the final manuscript.

CONFLICTS OF INTEREST

The authors declare no competing interests.

ACKNOWLEDGMENTS

This study was supported by the National Natural Science Foundation of China (81372039), the Natural Science Foundation of Liaoning Province (2017225003 and 2018108001), and the Science and Technology Foundation of Shenyang (F13-220-9-38).

REFERENCES

1. Singer, M., Deutschman, C.S., Seymour, C.W., Shankar-Hari, M., Annane, D., Bauer, M., Bellomo, R., Bernard, G.R., Chiche, J.D., Coopersmith, C.M., et al. (2016). The Third International Consensus Definitions for Sepsis and Septic Shock (Sepsis-3). JAMA *315*, 801–810.
2. Angus, D.C., and van der Poll, T. (2013). Severe sepsis and septic shock. N. Engl. J. Med. *369*, 2063.
3. Raj, S., Killinger, J.S., Gonzalez, J.A., and Lopez, L. (2014). Myocardial dysfunction in pediatric septic shock. J. Pediatr. *164*, 72–77.e2.
4. Brierley, J., and Peters, M.J. (2008). Distinct hemodynamic patterns of septic shock at presentation to pediatric intensive care. Pediatrics *122*, 752–759.
5. Weiss, S.L., Fitzgerald, J.C., Pappachan, J., Wheeler, D., Jaramillo-Bustamante, J.C., Salloo, A., Singhi, S.C., Erickson, S., Roy, J.A., Bush, J.L., et al.; Sepsis Prevalence, Outcomes, and Therapies (SPROUT) Study Investigators and Pediatric Acute Lung Injury and Sepsis Investigators (PALISI) Network (2015). Global epidemiology of pediatric severe sepsis: the sepsis prevalence, outcomes, and therapies study. Am. J. Respir. Crit. Care Med. *191*, 1147–1157.
6. Ho, J., Chan, H., Wong, S.H., Wang, M.H., Yu, J., Xiao, Z., Liu, X., Choi, G., Leung, C.C., Wong, W.T., et al. (2016). The involvement of regulatory non-coding RNAs in sepsis: a systematic review. Crit. Care *20*, 383.
7. Boon, R.A., Jaé, N., Holdt, L., and Dimmeler, S. (2016). Long Noncoding RNAs: From Clinical Genetics to Therapeutic Targets? J. Am. Coll. Cardiol. *67*, 1214–1226.
8. Trapnell, C., Williams, B.A., Pertea, G., Mortazavi, A., Kwan, G., van Baren, M.J., Salzberg, S.L., Wold, B.J., and Pachter, L. (2010). Transcript assembly and quantification by RNA-Seq reveals unannotated transcripts and isoform switching during cell differentiation. Nat. Biotechnol. *28*, 511–515.
9. Griffith, M., Griffith, O.L., Mwenifumbo, J., Goya, R., Morrissy, A.S., Morin, R.D., Corbett, R., Tang, M.J., Hou, Y.C., Pugh, T.J., et al. (2010). Alternative expression analysis by RNA sequencing. Nat. Methods *7*, 843–847.
10. Yang, N., Shi, X.L., Zhang, B.L., Rong, J., Zhang, T.N., Xu, W., and Liu, C.F. (2018). The Trend of β3-Adrenergic Receptor in the Development of Septic Myocardial Depression: A Lipopolysaccharide-Induced Rat Septic Shock Model. Cardiology *139*, 234–244.
11. Winkler, M.S., Rissiek, A., Priefler, M., Schwedhelm, E., Robbe, L., Bauer, A., Zahrte, C., Zoellner, C., Kluge, S., and Nierhaus, A. (2017). Human leucocyte antigen (HLA-DR) gene expression is reduced in sepsis and correlates with impaired TNFα response: A diagnostic tool for immunosuppression? PLoS ONE *12*, e0182427.
12. Wu, H., Liu, J., Li, W., Liu, G., and Li, Z. (2016). LncRNA-HOTAIR promotes TNF-α production in cardiomyocytes of LPS-induced sepsis mice by activating NF-κB pathway. Biochem. Biophys. Res. Commun. *471*, 240–246.
13. Qi, J., Qiao, Y., Wang, P., Li, S., Zhao, W., and Gao, C. (2012). microRNA-210 negatively regulates LPS-induced production of proinflammatory cytokines by targeting NF-κB1 in murine macrophages. FEBS Lett. *586*, 1201–1207.
14. Filgueiras, L.R., Jr., Martins, J.O., Serezani, C.H., Capelozzi, V.L., Montes, M.B., and Jancar, S. (2012). Sepsis-induced acute lung injury (ALI) is milder in diabetic rats and correlates with impaired NFkB activation. PLoS ONE *7*, e44987.
15. Jin, H., Fujita, T., Jin, M., Kurotani, R., Namekata, I., Hamaguchi, S., Hidaka, Y., Cai, W., Suita, K., Ohnuki, Y., et al. (2017). Cardiac overexpression of Epac1 in transgenic mice rescues lipopolysaccharide-induced cardiac dysfunction and inhibits Jak-STAT pathway. J. Mol. Cell. Cardiol. *108*, 170–180.
16. Lv, X., Zhang, Y., Cui, Y., Ren, Y., Li, R., and Rong, Q. (2015). Inhibition of microRNA-155 relieves sepsis-induced liver injury through inactivating the JAK/STAT pathway. Mol. Med. Rep. *12*, 6013–6018.
17. Li, Z., Jia, Y., Feng, Y., Cui, R., Miao, R., Zhang, X., Qu, K., Liu, C., and Zhang, J. (2019). Methane alleviates sepsis-induced injury by inhibiting pyroptosis and apoptosis: in vivo and in vitro experiments. Aging (Albany N.Y.) *11*, 1226–1239.
18. Girardot, T., Rimmelé, T., Venet, F., and Monneret, G. (2017). Apoptosis-induced lymphopenia in sepsis and other severe injuries. Apoptosis *22*, 295–305.
19. Cho, S.W., Xu, J., Sun, R., Mumbach, M.R., Carter, A.C., Chen, Y.G., Yost, K.E., Kim, J., He, J., Nevins, S.A., et al. (2018). Promoter of lncRNA Gene PVT1 Is a Tumor-Suppressor DNA Boundary Element. Cell *173*, 1398–1412.e22.

20. He, Y., Jing, Y., Wei, F., Tang, Y., Yang, L., Luo, J., Yang, P., Ni, Q., Pang, J., Liao, Q., et al. (2018). Long non-coding RNA PVT1 predicts poor prognosis and induces radioresistance by regulating DNA repair and cell apoptosis in nasopharyngeal carcinoma. Cell Death Dis. *9*, 235.

21. Rhodes, A., Evans, L.E., Alhazzani, W., Levy, M.M., Antonelli, M., Ferrer, R., Kumar, A., Sevransky, J.E., Sprung, C.L., Nunnally, M.E., et al. (2017). Surviving Sepsis Campaign: International Guidelines for Management of Sepsis and Septic Shock: 2016. Intensive Care Med. *43*, 304–377.

22. Zhou, J., Xiong, Q., Chen, H., Yang, C., and Fan, Y. (2017). Identification of the Spinal Expression Profile of Non-coding RNAs Involved in Neuropathic Pain Following Spared Nerve Injury by Sequence Analysis. Front. Mol. Neurosci. *10*, 91.

23. Wang, W., Gao, Z., Wang, H., Li, T., He, W., Lv, W., and Zhang, J. (2016). Transcriptome Analysis Reveals Distinct Gene Expression Profiles in Eosinophilic and Noneosinophilic Chronic Rhinosinusitis with Nasal Polyps. Sci. Rep. *6*, 26604.

24. Takasu, O., Gaut, J.P., Watanabe, E., To, K., Fagley, R.E., Sato, B., Jarman, S., Efimov, I.R., Janks, D.L., Srivastava, A., et al. (2013). Mechanisms of cardiac and renal dysfunction in patients dying of sepsis. Am. J. Respir. Crit. Care Med. *187*, 509–517.

25. Li, W., Zheng, Z., Chen, H., Cai, Y., and Xie, W. (2018). Knockdown of long non-coding RNA PVT1 induces apoptosis and cell cycle arrest in clear cell renal cell carcinoma through the epidermal growth factor receptor pathway. Oncol. Lett. *15*, 7855–7863.

26. Tseng, Y.Y., Moriarity, B.S., Gong, W., Akiyama, R., Tiwari, A., Kawakami, H., Ronning, P., Reuland, B., Guenther, K., Beadnell, T.C., et al. (2014). PVT1 dependence in cancer with MYC copy-number increase. Nature *512*, 82–86.

27. Colombo, T., Farina, L., Macino, G., and Paci, P. (2015). PVT1: a rising star among oncogenic long noncoding RNAs. BioMed Res. Int. *2015*, 304208.